RSC Advances

PAPER

View Article Online
View Journal | View Issue

Cite this: *RSC Adv.*, 2023, **13**, 14078

Comparison of plasma technology for the study of herbicide degradation†

Chonlada Bennett, *[a] Sawanya Ngamrung,[a] Vithun Ano,[a] Chanchai Umongno,[bc] Sugunya Mahatheeranont,[def] Jaroon Jakmunee,[deg] Mudtorlep Nisoa,[h] Komgrit Leksakul,[i] Choncharoen Sawangrat[i] and Dheerawan Boonyawan *[bc]

The study aimed to investigate the effects of two different plasma systems, including pinhole plasma jet and gliding arc (GA) plasma, for the degradation of herbicide, diuron, in plasma activated solutions (PAS). In the GA plasma system, air was used to generate plasma, however, Ar, oxygen and nitrogen at different gas compositions were compared in the pinhole plasma jet system. The Taguchi design model was used to study the effects of gas compositions. Results revealed that the pinhole plasma jet system was able to degrade over 50% of the diuron in 60 minutes. The optimal plasma generation condition for the highest degradation of diuron used pure Ar gas. The highest degradation percentage of herbicide in PAS corresponded to the lowest hydrogen peroxide (H_2O_2) content, nitrite concentration and electrical conductivity (EC) of the PAS. The diuron degradation products were identified as 3,4-dichloro-benzenamine, 1-chloro-3-isocyanato-benzene and 1-chloro-4-isocyanato-benzene *via* gas chromatography-mass spectrometry (GC-MS). The GA plasma system was not adequate for the degradation of herbicide in PAS.

Received 21st January 2023
Accepted 25th April 2023

DOI: 10.1039/d3ra00459g

rsc.li/rsc-advances

Introduction

Hazardous agricultural chemicals and their degradation residues are major concerns in the areas of food safety and public health. Thailand is considered as one of the world's largest producers of food and agricultural products.[1] Pesticides such as herbicides, insecticides and fungicides are often used to control weed and pest infestation to prevent the loss of crop yield. Intensive use and exposure to pesticides is a serious health problem and has considerable consequences to the environment.[2] Pesticide accumulation in water bodies due to runoff from agricultural areas or industrial sites pose a huge problem to the environment.[3] To tackle this issue, this study aims to investigate the use of plasma technology for the treatment of pesticide in water and to study their degradation pathways.

Diuron is a persistent herbicide that can be found in surface and ground water. It is used as a sterilant in soil, mildewcide in paints and stains, and algicide in fish production.[4,5] Diuron acts as an inhibitor of photosynthesis in microorganisms. It is also used in non-crop products for industrial purposes, such as formulations in wettable powders and suspension concentrates in paint.[6] According to the Environmental Protection Agency, a ban on the use of diuron was proposed in the US in 2022 due to carcinogenic effects. The degradation of diuron in the environment can occur through hydrolysis under pH of 5 over a period of 30 days. In water, the photodegradation may occur with a half-life of 43 days and 15 days after exposure to natural sunlight. Additionally, the photodegradation of diuron in deep soil may degrade with a half-life of 173 days.[7]

Various researchers have confirmed the effectiveness of plasma technology for the removal of chemicals from contaminated agricultural products, however, little is known about the reaction mechanisms. Free radicals are generated, which induce chemical reactions in chemical substances or microorganisms. The use of low-temperature plasma technology to decompose pesticide residues in food products to inhibit microorganisms has been incorporated due to the retainment

[a]*Agriculture and Bio Plasma Technology Center (ABPlas), Science and Technology Park, Chiang Mai University, Chiang Mai 50100, Thailand*
[b]*Plasma and Beam Physics Research, Faculty of Science, Chiang Mai University, Chiang Mai 50200, Thailand*
[c]*Department of Physics and Materials Science, Faculty of Science, Chiang Mai University, Chiang Mai 50200, Thailand*
[d]*Department of Chemistry, Faculty of Science, Chiang Mai University, Chiang Mai, 50200, Thailand*
[e]*Center of Excellence for Innovation in Chemistry, Faculty of Science, Chiang Mai University, Chiang Mai, 50200, Thailand*
[f]*Research Center on Chemistry for Development of Health Promoting Products from Northern Resources, Chiang Mai University, Chiang Mai, 50200, Thailand*
[g]*Center of Advanced Materials of Printed Electronics and Sensors, Materials Science Research Center, Faculty of Science, Chiang Mai University, Chiang Mai, 50200, Thailand*
[h]*School of Science, Walailak University, Nakhon Si Thammarat, 80160, Thailand*
[i]*Department of Industrial Engineering, Faculty of Engineering, Chiang Mai University, Chiang Mai 50200, Thailand*

† Electronic supplementary information (ESI) available. See DOI: https://doi.org/10.1039/d3ra00459g

of the freshness and colour of the agricultural products.[8] Highly reactive oxygen and nitrogen species are considered the prominent reactive chemical component for the decontamination of food.[9,10] Plasma-activated solution (PAS) has emerged as a novel medium for the non-toxic chemical decontamination of agricultural products. In PAS, the active particles generated by plasma react with water molecules to initiate a cascade of chemical reactions. PAS is advantageous as it can be used to remove pesticides in fruits and vegetables on a large-scale non-homogeneous surface.[11] The generation of plasma produces primary and secondary reactive species, including hydroxyl radicals, atomic oxygen, ozone, superoxide, H_2O_2, atomic nitrogen and nitric oxides. The reactive species have broad applications such as plant germination enhancement, microbial inactivation, and organic compound removal. The nitrate and nitrite ions in PAS are toxic to cell and possess strong bacterial disinfection.[12] Free hydroxyl radicals are reported to effectively degrade harmful chemicals. Depending on the process parameters, the formation of plasma *via* different systems will generate different types of reactive species at various concentration.[13]

The aim of this research was to observe the degradation mechanism of the herbicide, diuron, *via* pinhole plasma jet and GA plasma treatment. The degradation of herbicide in plasma activated solution (PAS) *via* pinhole plasma jet plasma was investigated using Taguchi design. The identification of chemical structures in the degradation pathway was determined using gas chromatography mass spectrometry (GC-MS) and high-performance liquid chromatography coupled with diode array detector (HPLC-DAD). Response surface methodology was used to analyse the degradation percentage of diuron as well as the physicochemical properties of PAS.

Materials and method

Chemicals and instruments

Diuron standard (98.7% purity) was purchased from Dr Ehrenstorfer (LGC Labor GmbH, Augsburg, Germany). Analytical grade MeOH, HPLC grade MeOH, hydrochloric acid, potassium nitrate, sodium nitrite, potassium chloride and sodium thiosulfate were purchased from RCI Labscan (RCI Labscan Ltd., Bangkok, Thailand). HI3874-0 nitrate reagent, HI3873-0 nitrite reagent and potassium iodide solution was obtained from HANNA instruments (Hanna Instruments Inc., Woonsocket, RI, USA). Deionised water was obtained from a MilliQ UV-Plus water purification system (Millipore Corp., Billerica, MA). Digital thermometer and pH meter used HANNA instruments (Hanna Instruments Inc., Woonsocket, RI, USA). Oxidation–reduction potential (ORP) and electrical conductivity (EC) meter used a Seven Compact Duo S213 (Mettler-Toledo, Greifensee, Switzerland). Nitrate and nitrite concentration was measured using a UV-Vis spectrophotometer (EMC-11-UV, EMCLAB Instruments GmbH, Duisburg, Germany). Hydrogen peroxide content was determined *via* the iodometric titration method. Argon (Ar), nitrogen (N_2) and oxygen (O_2) gas were obtained from Lanna Industrial Gases Co., Ltd. (Chiang Mai, Thailand).

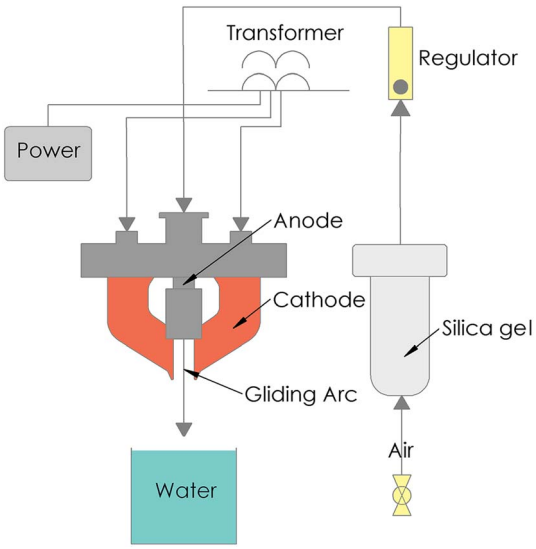

Fig. 1 Schematic diagram of gliding arc system.

Plasma systems

In the GA system, plasma was generated through air using a high-voltage power source. A 125 watt neon transformer with a voltage of 15 kV was used to discharge plasma through a high-voltage copper electrode. Plasma was discharged 1.5 cm from the DI water surface. Silica gel was used to control the humidity of the air entering the GA system. A flow rate of 1 and 3 L min^{-1} air was used. A schematic diagram of the GA system is shown in Fig. 1. In pinhole plasma jet, plasma was discharged through a perforated borosilicate glass tube, allowing the plasma to interface with the flow of DI water. A 125 watt neon transformer rated at 15 kV was used as the high-voltage power supply. Plasma was generated by a neon transformer using a high-voltage electrode made of 304 L stainless steel sheet with a diameter of 2.5 mm. A constant flow of Ar gas was fixed at 3 L min^{-1}. A schematic diagram of the pinhole plasma jet system

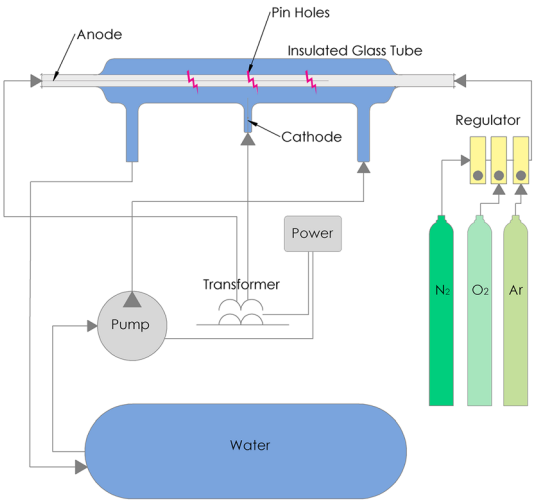

Fig. 2 Schematic diagram of pinhole plasma jet system.

Table 1 Taguchi design table for diuron degradation *via* pinhole plasma jet system

	Level		
Parameter	−1	0	1
N_2	0	10	20
O_2	0	10	20

Table 2 Diuron chemical information

Formula	Molecular weight	Solubility in water	IUPAC name
$C_9H_{10}Cl_2N_2O$	233.095	0.042 g L^{-1} at 25 °C	3-(3,4-Dichlorophenyl)-1,1-dimethylurea

is shown in Fig. 2. Additionally, N_2 and O_2 gas were introduced to the constant flow of Ar as individual and mixture of gases at various concentrations following the Taguchi method design.

Taguchi method for herbicide degradation in PAS

The degradation of herbicide *via* pinhole plasma was studied using a 3-level Taguchi design model with 2 factors, 3 replicates and 27 runs (Table 1). The herbicide solution was prepared using 10.00 ppm of diuron standard in 500 mL of DI with 25% MeOH. Methanol was added to aid the complete dissolution of the standard. The herbicide solution was circulated through the pinhole plasma jet system for 60 min. The concentration of herbicide before and after the plasma treatment was quantified *via* high performance liquid chromatography coupled with a diode array detector (HPLC-DAD). The herbicide and its degradation by-product were identified *via* gas chromatography mass spectrometry (GC-MS). The physicochemical properties of the herbicide solution after the plasma treatment were determined. These include pH, temperature, ORP, EC, nitrate concentration, nitrite concentration, and H_2O_2 concentration. Results were evaluated using response surface methodology (RSM) where the optimal plasma condition for herbicide degradation was determined using Minitab software version 18.0 (Minitab LLC., Pennsylvania, PA). Significant terms were analysed using the full quadratic model at $p < 0.05$. Analysis of variance (ANOVA) was used to determine the lack of fit of the model. Statistical significances were analysed using *post hoc* Tukey's test *via* SPSS version 17.0 (SPSS Inc., Chicago, IL).

High performance liquid chromatography

The analysis of diuron was performed using a 1260 series HPLC (Agilent Technology CO., Lts., CA, USA) equipped with diode array detector (DAD). Diuron standard (98.7% purity; Dr Ehrenstorfer, LGC Labor GmbH, Augsburg, Germany) was quantified using gradient elution consisting of methanol (line A) and DI (line B). Samples and standards were separated using a Zorbax C18 column (2.1 mm × 150.0 mm, 4.5 μm) with the injection volume of 5.0 μL and a flow rate of 1.2 mL min^{-1}. The initial gradient was 10% B and decreased to 0% B (1.0 min). The solvent was held at 0% B until 2.8 min and re-equilibrated to 10% B to obtain a total run time of 3.0 min. The column temperature was constant at 30.0 °C. The wavelength maxima of diuron was found at 254 nm.

Gas chromatography mass spectrometry

The identification of diuron and its degradation product was determined using GC-MS equipped with a DB-5 column (30.0 m × 0.25 mm, 0.25 μm) at flow rate of 1.2 mL min^{-1}, injection volume of 5.0 μL and split ratio of 1 : 10. The initial column temperature was held at 120.0 °C for 4.0 min and ramped at 12.5 to 280.0 °C. The final temperature was held at 280.0 °C for 3.0 min and the total run time was 16 min. The chemical information of diuron is found in Table 2.

Ion chromatography

Plasma activated DI water was analysed using an ion chromatography system (Integrion RFIC, Thermo Fisher Scientific, Waltham, MA) coupled with a conductivity detector. A Dionex IonPac™ AS18 anion exchange column (4 × 250 mm) maintained at 30 °C was employed as the stationary phase. A flow rate of 1 mL min^{-1} and injection volume of 250 μL was used to carry out the anion test for fluoride, chloride, nitrite, bromide, sulphate, nitrate, and phosphate ions, respectively.

Result and discussions

Diuron degradation *via* GA plasma system

In the generation of PAS *via* the GA plasma system, the dominant air molecules (such as N_2 and O_2) were ionized and dissociated by the strong electric field induced by the high energy electrons.[11] The ionization and dissociation equation of the reaction is described by the following reaction equation (eqn (1)):

$$e^- + N_2 \rightarrow e^- + N_2^* \quad (1)$$

An important advantage of the GA plasma device is the arc area, which can lead to high-density ionisation. Copper electrodes were used in this study for the generation of reactive nitrogen and reactive oxygen species (RONS) through ambient air. The custom-made GA plasma unit had a curved-sharp copper electrode as the high-voltage electrode for the power supply. The physicochemical properties of PAS after GA plasma discharge are displayed in Fig. 3. It was shown that with increasing volume, the temperature of the solution after the plasma treatment was not significantly different. EC and ORP values were decreased with increasing water volume. The pH was ranged from 2.7 to 3.4 and was increased with increasing water volume. The highest nitrite concentration was found at 75 mL of DI water. However, the lowest nitrite and nitrate concentration was found at 100 mL of DI water. A decrease in nitrite concentration was reported to be attributed to the peroxynitration process that occurs at pH lower than 4.[14] This is

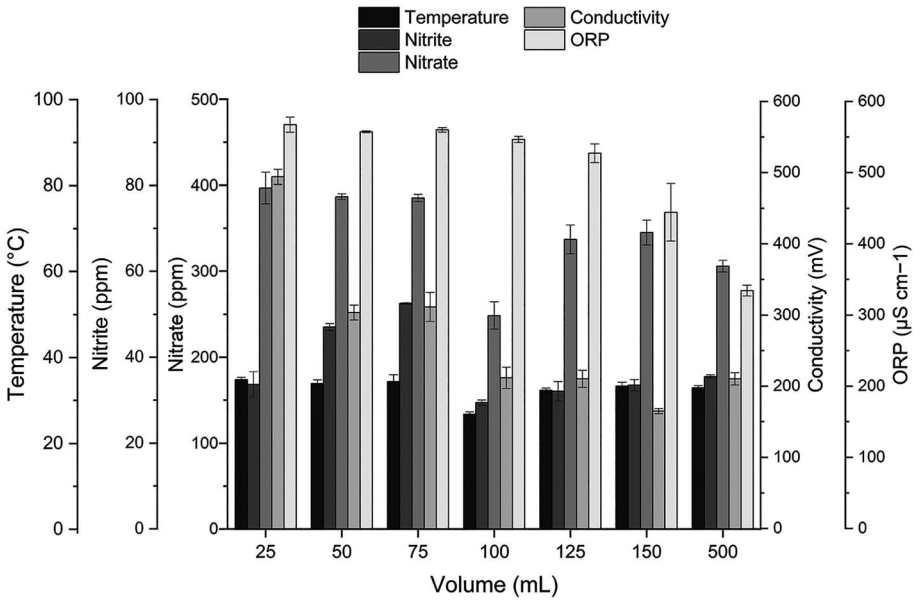

Fig. 3 The physicochemical properties of PAS after gliding arc discharge.

because nitrites are not stable under acidic conditions (pH < 3.5). The reaction of nitrite is formed through the dissolution of NO_x species from the air discharge plasma into the water, followed by a decrease in pH. The shift in pH is originated from the formation of nitric and nitrous acid (HNO_3 and HNO_2) by the reaction of NO and NO_2 *via* the following chemical reactions (eqn (2)–(6)).[15]

$$N_2 + O_2 + e^- \rightarrow 2NO + e^- \quad (2)$$

$$2NO + O_2 \rightarrow 2NO_2 \quad (3)$$

$$H_2O + e^- \rightarrow OH + H + e^- \quad (4)$$

$$NO_2 + OH \rightarrow HNO_3 \quad (5)$$

$$NO + OH \rightarrow HNO_2 \quad (6)$$

Above the water surface, the electron impact can also produce atomic oxygen (O) and OH by dissociative excitation of the water vapor (eqn (7) and (8)). Both O and OH are transient chemical species that have very strong oxidative properties compared to neutral oxidant molecules.[16]

$$e^- + O_2 \rightarrow e^- + O^1P + O^1D \quad (7)$$

$$e^- + H_2O \rightarrow e^- + H^* + OH^* \quad (8)$$

Both reactive oxygen species (ROS) and reactive nitrogen species (RNS) such as ozone, H_2O_2 and nitrite are generated during GA plasma production in the gas phase.[16] Concerning the degradation of herbicide, ESI Fig. 1† shows the HPLC chromatogram of the diuron standard before and after the treatment *via* GA plasma. The amount of herbicide solution (100 and 500 mL), treatment time (30 and 90 min) and flow rate (1 and 3 L min^{-1}) were investigated. Results showed that the GA plasma system was not able to degrade the diuron herbicide in solution, however, a slight increase in diuron concentration after the plasma treatment was observed. The slight increase in diuron concentration was due to the increased dissolution of

Table 3 Degradation percentage of diuron *via* Taguchi design model *via* pinhole plasma jet[a]

Treatment	N_2 (%)	O_2 (%)	Degradation percentage	Hydrogen peroxide (ppm)	Nitrite content (ppm)	Nitrate content (ppm)
1	0	0	50.71 ± 7.40^{a}	5.56 ± 0.19^{c}	0.039 ± 0.004^{c}	4.47 ± 0.30^{de}
2	0	10	40.94 ± 6.50^{ab}	17.40 ± 0.42^{a}	0.038 ± 0.003^{c}	3.49 ± 0.29^{e}
3	0	20	39.62 ± 0.47^{b}	15.12 ± 3.27^{ab}	0.050 ± 0.008^{c}	6.78 ± 0.44^{c}
4	10	0	46.00 ± 2.96^{ab}	9.45 ± 1.64^{c}	1.836 ± 0.190^{b}	8.83 ± 0.29^{b}
5	10	10	39.89 ± 2.50^{b}	17.01 ± 0.00^{a}	0.066 ± 0.006^{c}	6.00 ± 0.49^{cd}
6	10	20	39.36 ± 2.52^{b}	17.01 ± 0.00^{a}	0.093 ± 0.033^{c}	6.68 ± 0.14^{c}
7	20	0	47.20 ± 1.23^{ab}	10.39 ± 1.64^{bc}	2.345 ± 0.361^{a}	12.56 ± 0.34^{a}
8	20	10	39.82 ± 1.76^{b}	17.03 ± 0.03^{a}	0.045 ± 0.007^{c}	4.87 ± 0.91^{de}
9	20	20	39.50 ± 0.56^{b}	15.23 ± 3.08^{ab}	0.059 ± 0.006^{c}	6.87 ± 1.12^{c}

[a] Values expressed as the mean ± standard deviation derived from triplicate samples ($n = 3$). Significant differences ($P < 0.05$) within the same column are represent by lowercase superscript letters.

Table 4 Physicochemical properties of herbicide solution after pinhole plasma jet treatment[a]

Treatment	N_2 (%)	O_2 (%)	Conductivity (μS cm^{-1})	ORP (mV)	Temperature (°C)	pH
1	0	0	24.30 ± 0.85^{d}	340.0 ± 19.3^{b}	30.1 ± 1.0*	4.63 ± 0.19^{b}
2	0	10	48.93 ± 1.10^{b}	441.7 ± 7.5^{a}	28.6 ± 1.4*	3.97 ± 0.04^{cd}
3	0	20	55.02 ± 0.47^{b}	446.0 ± 13.1^{a}	28.7 ± 0.3*	3.91 ± 0.06^{cd}
4	10	0	33.81 ± 2.26^{cd}	320.0 ± 3.6^{b}	29.8 ± 0.3*	5.12 ± 0.10^{a}
5	10	10	58.37 ± 4.53^{b}	421.3 ± 8.5^{a}	28.7 ± 0.8*	3.87 ± 0.07^{cd}
6	10	20	72.44 ± 3.79^{a}	427.7 ± 4.5^{a}	28.0 ± 0.9*	3.71 ± 0.07^{d}
7	20	0	35.82 ± 2.19^{c}	307.3 ± 18.8^{b}	29.6 ± 0.8*	5.22 ± 0.07^{a}
8	20	10	53.03 ± 2.53^{b}	415.0 ± 6.1^{a}	29.3 ± 0.6*	4.01 ± 0.13^{c}
9	20	20	73.36 ± 9.10^{a}	442.7 ± 22.8^{a}	29.5 ± 0.9*	3.77 ± 0.11^{cd}

[a] Values expressed as the mean ± standard deviation derived from triplicate samples ($n = 3$). Significant differences ($P < 0.05$) within the same column are represented by lowercase superscript letters. No significant difference between the means of the data is represented by an asterisk.

the compound caused by the plasma treatment and the increase acidity of the PAS. This is because the diuron standard had very low solubility in water before the plasma treatment but was still present in the soluble as an undetectable form. The slight increase in diuron concentration was observed after the plasma treatment due to the increased dissolution of the compound where the increased acidity of the PAS was caused by the plasma treatment. In the presence of OH radicals, the structure of diuron can exist as a radical which cannot be detected by HPLC. However, in the presence of H radicals, the diuron compound is protonated into the non-radical structure, thereby increasing the concentration.[17] Furthermore, the breakage and dissociation of chemical bonds were not provoked. In the literature, the structural changes of organic compounds *via* plasma treatment such as diuron is described to be modified through hydrogen abstraction. Through this process, the carboxyl (–COOH) or hydroxyl group (–OH) is transformed into radicals such as RCOO$^{\bullet}$ and R–O$^{\bullet}$, respectively. The H atom of methyl is replaced with a hydroxyl group.[18]

Diuron degradation *via* pinhole plasma jet system

The physicochemical properties of diuron PAS after pinhole plasma treatment is summarised in Tables 3 and 4. ESI Fig. 2† shows the HPLC chromatogram of diuron standard before and after the pinhole plasma jet treatment. The highest degradation percentage (50.71 ± 7.40%) of diuron was obtained from the treatment using pure Ar gas (T1). The addition of N_2 and O_2 gas to the constant flow of Ar was not able to increase the degradation percentage of diuron. The increase of individual N_2 and O_2 gas concentration correlated to the decrease in diuron degradation percentage. The mixture of nitrogen and oxygen at different concentration compositions did not have a significant effect on the degradation of diuron in solution. It was previously reported that the N_2 plasma was less effective in the decontamination of food products as well as anti-microbial and anti-bacterial activity than that of Ar gas. Noble gases such as Ar was described to have high thermal conductivity, low operating discharge voltage at atmospheric pressure and abundant in charged particles.[19] Ar plasma was reported to induce methylation reactions in soybean.[20] Interestingly, T1 corresponded to the lowest H_2O_2 concentration (5.56 ± 0.19 ppm), nitrite concentration (0.039 ± 0.004 ppm) and EC (24.30 ± 0.85 μS cm^{-1}) of the herbicide solution after the plasma treatment. Contrary, the dissociation of water by Ar is described to form OH radicals ($^{\bullet}$OH) through the dissociative excitation of the water molecules by the excited Ar atom (Ar*).[21] The production of radicals from the pure Ar gas can be described *via* the following reaction equations (eqn (9)–(11)). It could be suggested that the low H_2O_2 content found in T1 may have been due to the involvement of $^{\bullet}$OH in the degradation mechanism of the herbicide, resulting in less H_2O_2 concentrations.

$$Ar + e \rightarrow Ar^* + e \quad (9)$$

$$Ar^* + H_2O \rightarrow Ar + H^{\bullet} + OH^{\bullet} \quad (10)$$

$$OH^{\bullet} + OH^{\bullet} \rightarrow H_2O_2 \quad (11)$$

When O_2 is introduced into the system (T2 and T3), the EC (48.93 ± 1.10 μS cm^{-1} and 55.02 ± 0.47 μS cm^{-1}, respectively) and ORP (441.7 ± 7.5 mV and 446.0 ± 13.1 mV, respectively) of the PAS was relatively higher than that of T1. Higher H_2O_2 content (17.40 ± 0.42 ppm and 15.12 ± 3.27 ppm, respectively) was observed which correlated to the lower degradation percentage of the herbicide. The acidity of the solution was increased (3.97 ± 0.04 and 3.91 ± 0.06) in comparison to T1 (4.63 ± 0.19). This is due to the strong electronegativity of the oxygen and the limited amount of nitrogen available.[22] Furthermore, the collision reaction of the oxygen and excited Ar atom occurs to produce singlet oxygen atoms (eqn (12)) which can bombard further with water molecules to obtain hydroxyl radicals (eqn (13)) and H_2O_2 (eqn (11)).[23]

$$Ar^* + O_2 \rightarrow O + O \quad (12)$$

$$O + H_2O \rightarrow 2OH^{\bullet} \quad (13)$$

$$Ar^* + N_2 \rightarrow Ar + 2N \quad (14)$$

$$2N + 2H_2O \rightarrow 2OH^{\bullet} + N_2 \quad (15)$$

In the case of Ar + N_2, the main reactive species was reported as H_2O_2 and nitrate (eqn (14) and (15)).[22,24] This was in

accordance with our results where T4 and T7 obtained the highest nitrite (1.836 ± 0.190 ppm and 2.345 ± 0.361 ppm, respectively) and nitrate (8.83 ± 0.29 ppm and 12.56 ± 0.34 ppm, respectively) concentration with statistical significance. The Ar + N_2 obtained the second highest diuron degradation percentage, after that of T1. Similarly, the concentration of H_2O_2 was the second and third lowest value with significant differences. The treatments (T5–T9) employing the mixture of N_2 and O_2 correlated to the low percentage of diuron degradation and the highest H_2O_2 and nitrite concentration, with statistical significance. T6 and T9 obtained to the highest EC (72.44 ± 3.79 and 73.36 ± 9.10 μS cm^{-1}, respectively) of the PAS and lowest pH (3.71 ± 0.07 and 3.77 ± 0.11, respectively) with statistical difference. It is cited in the literature that the high oxidation potential and acidic environment of PAS are important factors in the degradation efficiency of pesticides.[25] In our study, the highest degradation of pesticides occurred around a pH of 5. As the pH decreased from 5 to 3, the degradation efficiency of the PAS decreased. The pH of PAS is reported as a crucial factor for the degradation of pesticide, inducing hydrolysis reaction.[26] The decrease in pH is reported to minimise the hydrolysis reaction due to the solubilization of nitrogen oxides. In T4–T9, the decrease in H^+ corresponded to the increase of nitrogen species and decrease of oxygen species. Furthermore, plasma gas containing both N_2 and O_2 is considered to favour the formation of nitrogen oxides promoting the production of nitrogen dioxide. The dissolution of nitrogen oxides into water and the reaction of nitrogen oxide radical as well as nitrogen dioxide radical to produce dinitrogen trioxide is described by the reaction in eqn (16). The decrease in pH arising from the subsequent dissociation of dinitrogen trioxide is described by the reaction eqn (17). It was reported that the radicals are formed directly in the plasma region.[22]

$$NO^{\cdot} + NO_2^{\cdot} \rightarrow N_2O_3 \quad (16)$$

$$N_2O_3 + H_2O \rightarrow 2NO_2^- + 2H^+ \quad (17)$$

Response surface methodology for diuron degradation

The optimisation of diuron degradation was conducted using a Taguchi design model with the variation in N_2 and O_2 gas composition as the independent variables. Significant terms were analysed using the full quadratic model which obtained the following equation (eqn (18)):

$$\text{Degradation} = 51.41 - 0.0117N_2 - 0.1338O_2 + 0.000058N_2^*N_2 + 0.000426O_2^*O_2 + 0.000019N_2^*O_2 \quad (18)$$

The analysis of variance is summarised in Table 5. The model summary obtained a low standard error of the regression ($S = 1.67474$) implying high accuracy. The lack-of-fit was found to be non-significant at 0.05 significant level suggesting no evidence that the model does not fit the data. The coefficient of determination (R^2) was 0.9261, attributing the closeness of fit of the response variable to the regression model. The R^2 adjusted and predicted values were 0.8933 and 0.8265, respectively. This indicated that the data fits the model well and is able to predict values outside of the response model. The linear and squared effects of oxygen was found to be significant whereas the effects of nitrogen were not statistically significant at $p < 0.05$. The interaction of nitrogen and oxygen was also determined to be non-significant. This was evident in our preliminary experiment which demonstrated that the mixture of oxygen and nitrogen gas had little or no effects to the degradation percentage. The Taguchi design model was thus chosen in this study so that the effects of single gas compositions were the principal parameters. The obtained coefficients suggested that the addition of oxygen gas had a negative effect on the degradation percentage of diuron. The increase of oxygen gas composition did not increase the degradation efficacy of diuron but was shown to decrease the degradation percentage of diuron with significant differences. Previously, the photolysis of diuron was studied which demonstrated that the major degradation pathway is resulted from the photoheterolysis process where the substitution of chlorine by hydroxyl group is involved *via* $^{\cdot}OH$.[27] The effects of H_2O_2 on the degradation of diuron was investigated by Feng *et al.* Corresponding to our results, it was found that the degradation percentage of diuron (85%) was increased with increasing H_2O_2 but only at low concentrations. However, when the concentration of H_2O_2 was increased further, the degradation efficiency dramatically decreased (58–65%) with increasing H_2O_2 concentrations.[28] In view of this, it was concluded that the main reactive species in the degradation of diuron was due to the OH radicals. Plasma treatments of PAS obtaining a low dosage of H_2O_2 ultimately improved the degradation efficiency of diuron as less $^{\cdot}OH$ was consumed into H_2O_2.

Table 5 Analysis of variance for the optimisation of diuron degradation *via* pinhole plasma jet[a]

Source	DF	Adj. SS	Adj. MS	*F*-Value	*P*-Value
Model	8	632.745	79.093	28.20	0.000
Blocks	3	206.442	68.814	24.53	0.000
Linear	2	189.541	94.770	33.79	0.000
N_2	1	0.989	0.989	0.35	0.560
O_2	1	189.174	189.174	67.45	0.000
Square	2	101.758	50.879	18.14	0.000
$N_2^*N_2$	1	1.782	1.782	0.64	0.436
$O_2^*O_2$	1	100.433	100.433	35.81	0.000
2-Way interaction	1	0.383	0.383	0.14	0.716
$N_2^*O_2$	1	0.383	0.383	0.14	0.716
Error	18	50.486	2.805		
Lack-of-fit	8	20.183	2.523	0.83	0.595
Pure error	10	30.302	3.030		
Total	26	683.230			

[a] $R^2 = 0.9261$, adjusted $R^2 = 0.8933$, predicted $R^2 = 0.8265$; $S = 1.67474$; DF, degrees of freedom; SS, sum of squares; MS, mean square; *P* level < 0.05 indicates that the model terms are significant.

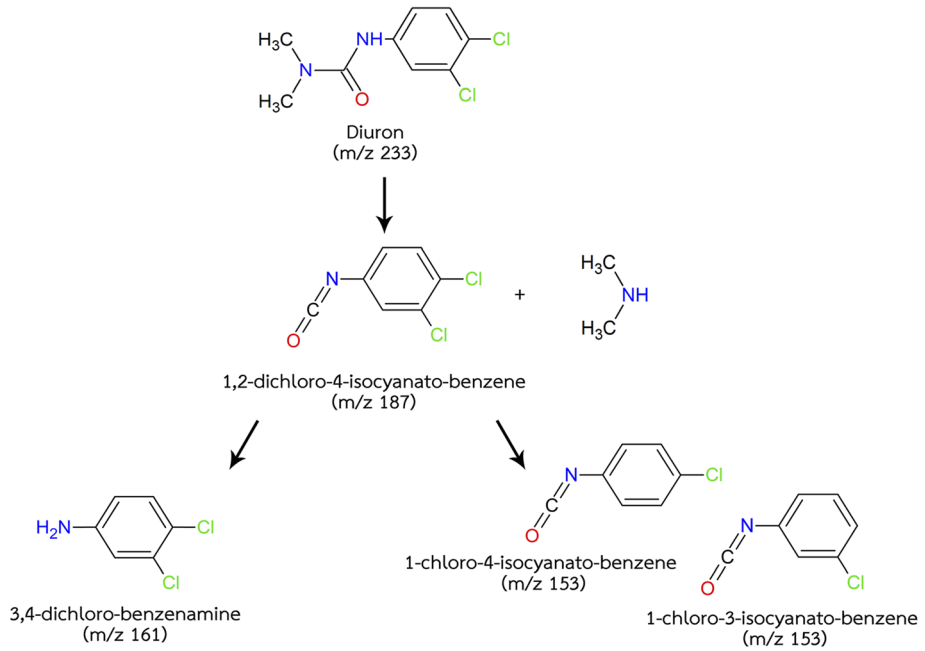

Fig. 4 Predicted degradation pathways for diuron after pinhole plasma jet treatment.

Diuron degradation mechanistic pathway

The mechanism of diuron degradation was analysed using GC-MS. The chromatogram in ESI Fig. 3† shows the comparison of diuron standard before and after pinhole plasma jet treatment. The metabolic pathway for the degradation of diuron have been reported through several mechanisms, including (i) oxidation, (ii) hydroxylation, (iii) dichlorination, and (iv) hydrolysis.[29,30] According to the GC-MS, diuron standard obtained 3 peaks at 8.0, 9.4 and 12.2 min corresponding to 1,2-dichloro-4-isocyanato-benzene (peak 3), 3,4-dichloro-benzenamine (peak 4) and 3-(3,4-dichlorophenyl)-1,1-dimethylurea (diuron; peak 5), respectively. After the plasma treatment, the diuron standard obtained two additional peaks identified as 1-chloro-3-isocyanato-benzene (peak 1) and 1-chloro-4-isocyanato-benzene (peak 2). It was evident from the GC-MS chromatogram that the amount of diuron (peak 5) and 1,2-dichloro-4-isocyanato-benzene (peak 3) was decreased after the treatment of plasma. The predicted degradation pathway for herbicide solution containing diuron standard is depicted in Fig. 4. The predicted pathway was in accordance with the research published by Giacomazzi *et al.*[31] and Temgoua *et al.*[30] The mass spectrum of diuron possessed protonated molecular ion $[M + H]^+$ at *m*/*z* 232.9 and fragmented ions at *m*/*z* 187.9 due to the loss of dimethylamine (45 Da). The breakage of C–N bond corresponding to the loss of dimethylamine may have occurred by the action of hydroxyl free radicals (˙OH) as they are reported to degrade organics *via* free radical reactions. Similar hydroxylation of the aromatic ring was observed during photocatalytic degradation.[29] The mass spectrum of 1,2-dichloro-4-isocyanato-benzene exhibited protonated molecular ion $[M + H]^+$ at *m*/*z* 186.9 and fragmented ions at *m*/*z* 158.9 suggesting the loss of C=O bond (28 Da) and *m*/*z* 124.0 due to the loss of chlorine molecule (36 Da). The peak at *m*/*z* 124.0 showed a larger M + 2 peak which is 2 mass units greater than the parent peak suggesting the presence of chlorine. The dechlorination of 1,2-dichloro-4-isocyanato-benzene was occurred to obtain the minor products, 1-chloro-3-isocyanato-benzene and 1-chloro-4-isocyanato-benzene. The substitution of chlorine on the aromatic ring with hydroxyl group was observed in some articles.[32] This was not present in our study, however, the hydrolysis reaction mechanism to obtain 3,4-dichloro-benzenamine was observed. Furthermore, Fenoll and co-worker reported that the hydrolysis reaction mechanism to obtain 3,4-dichloro-benzenamine could also be a result of the direct hydrolysis of diuron, disinvolvement of the other degradation compounds.[33] The mass spectrum of 3,4-dichloro-benzenamine revealed protonated molecular ion $[M + H]^+$ at *m*/*z* 160.9 and fragmented ions at *m*/*z* 143.8 resulting from the loss of OH (17 Da). Additionally, the mass spectrum of 1-chloro-3-isocyanato-benzene and 1-chloro-4-isocyanato-benzene showed protonated molecular ion $[M + H]^+$ at *m*/*z* 153.0. The presence of chlorine molecules was also present in the mass spectrum of 1-chloro-3-isocyanato-benzene and 1-chloro-4-isocyanato-benzene where a large M + 2 peak was observed at *m*/*z* 155.0. Other researchers have reported the hydrolytic dechlorination of the chlorine molecule into hydroxyl group.[30] This was observed in electrochemical degradation of diuron, however, the environmental degradation of diuron was similar to our results. The presence of single chlorine molecule attached to the benzene ring was recognised in the environmental degradation pathway. The degradation of diuron into 3,4-dichloro-benzenamine has been reported by many researchers through several mechanisms. These include direct and indirect photodegradation, abiotic degradation in water and aerobic degradation by fungi.[32,34,35] The common microbial degradation pathway for diuron is the transformation to 3,4-dichloro-benzenamine and metabolized

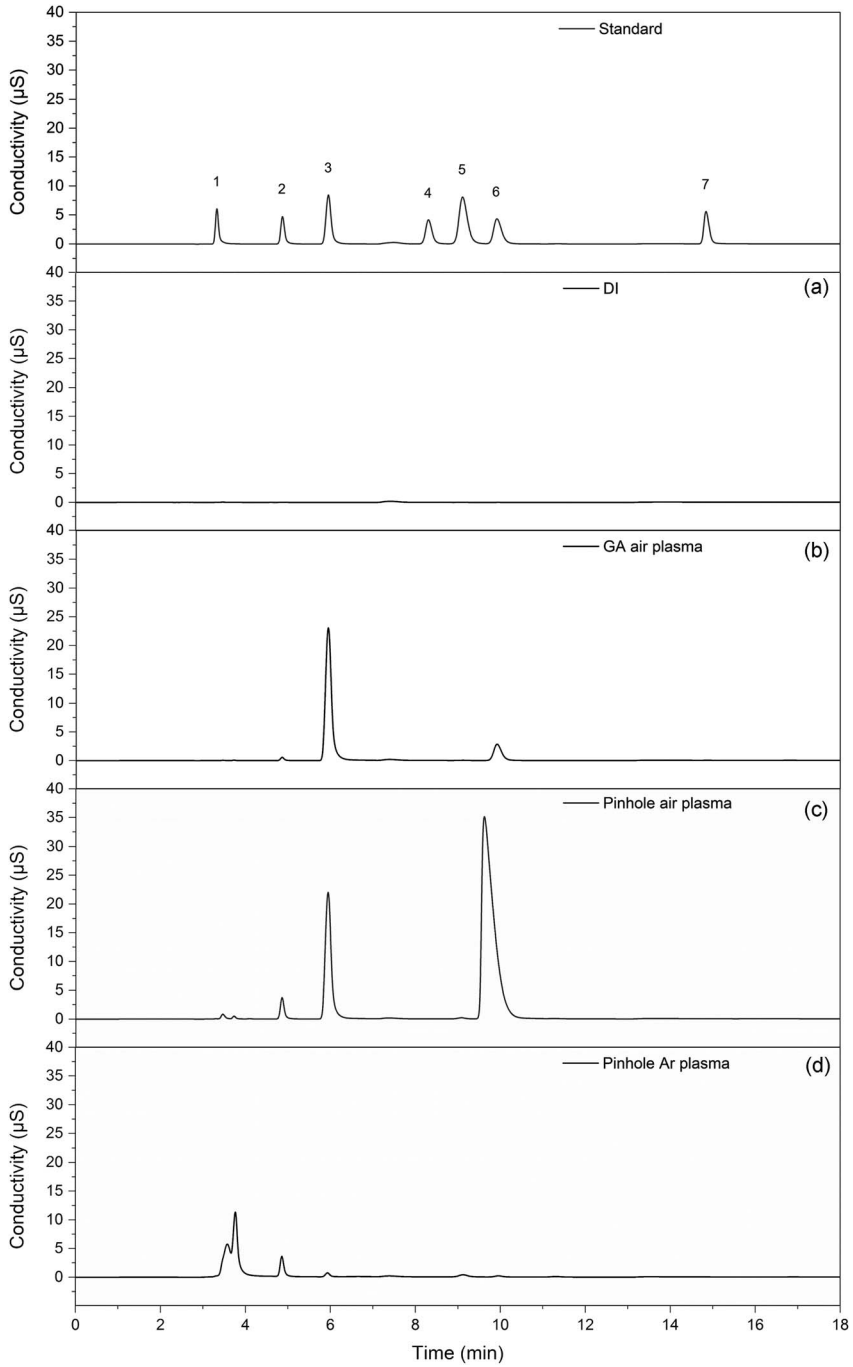

Fig. 5 Comparison of ions in DI water after pinhole plasma jet and gliding arc plasma treatment *via* ion chromatography (peak identifications; fluoride (1), chloride (2), nitrite (3), bromide (4), sulphate (5), nitrate (6), and phosphate (7)).

further through two different metabolic pathways: dehalogenation and hydroxylation, which can further degrade *via* cooperative metabolism.[36] Some authors suggest that the degradation products of diuron is more harmful to the environment than the parent compound.[37]

Comparison of PAS *via* GA and pinhole plasma jet systems

Ions in solutions can exist in several different forms depending on the pH of the solution. The analysis of ions in PAS from the GA and pinhole plasma jet systems was analysed using ion chromatography. Plasma was discharged using air and Ar gas to 500 mL of DI water. The chromatogram in Fig. 5 shows a comparison of the different ions in pure DI water (Fig. 5a), DI water after GA air plasma (Fig. 5b), DI water after pinhole air plasma (Fig. 5c) and DI water after pinhole Ar plasma (Fig. 5d). It was evident that the highest concentration of nitrate concentration was obtained from the pinhole air plasma (58.92 ppm) followed by the GA air plasma treatment (3.31 ppm), pinhole Ar plasma (0.27 ppm) and pure DI water (0.06 ppm),

respectively. The concentration of nitrite from the GA air plasma treatment (15.65 ppm) was relatively higher than that of the pinhole air plasma (14.77 ppm). In GA plasma systems, the direct electron impact dissociation of N_2 is much slower than that of O_2, where the major intermediate product is the atomic oxygen (O*). The electron collision with N_2 leads to the formation of various excited N_2 molecules. The generation of RONS in the propagation phase is described through the following equations (eqn (19)–(24)):[38]

$$N_2^* + O_2 \rightarrow N_2 + O^{\cdot} + O^{\cdot} \quad (19)$$

$$O^{\cdot} + O_2 + M \rightarrow O_3 + M \quad (20)$$

$$O^{\cdot} + O_2 \rightarrow NO + O^{\cdot} \quad (21)$$

$$O^{\cdot} + N_2 \rightarrow NO + N^{\cdot} \quad (22)$$

$$NO + O^{\cdot} + M \rightarrow NO_2 + M \quad (23)$$

$$O_3 + NO \rightarrow O_2 + NO_2 \quad (24)$$

where M is the neutral air molecule in the discharge volume. Furthermore, the nitrate–nitrogen species are generated in the water solution from the dissolved radicals (eqn (21)–(24)) following *via* the chemical reactions in eqn (25) and (26).

$$NO_2(aq) + NO_2(aq) + H_2O \rightarrow NO_2^* + NO_3^* + 2H^+ \quad (25)$$

$$NO(aq) + NO_2(aq) + H_2O \rightarrow 2NO_2^* + 2H^+ \quad (26)$$

GA plasma can produce both thermal and nonthermal plasma where the arc is generated in the gap between the two electrodes, allowing it to produce high amounts of heavy reactive species in humid air.[39] Consequently, this makes the system very suitable for the food industry as the nonthermal nature of the plasma causes minimal impact on the nutritional, physical and chemical characteristic of the food product.[40] However, the reactive species generated are short-lived and is more applicable for surface treatments such as the bombardment of ROS and RNS to provoke surface etching resulting in cell death of microorganisms.[41] In contrast, the efficacy of the plasma jet system has been reported for wastewater treatment such that the reactive species are described to decontaminate and degrade chemicals from wastewater and food processing industries.[42] This is mainly accredited to the interaction of singlet oxygen and hydroxyl radicals which was found to be the significant reactive species for pesticide degradation.[26] In GA, the production of hydroxyl radicals is believed to be due to the electron-induced dissociation of water vapour in open air. However, the radical formed breakdown rapidly due to the turbulent air flow.[43] From this, it was concluded that the degradation of herbicide *via* the GA plasma system in this work was not achieved. It was noted that the chemical reactions of various reactive species could have attributed to the degradation of herbicide differently. The difference in plasma due to the discharge characteristics (GA and pinhole plasma jet), input parameter (power and voltage) and gas flow could have consequently affected the efficacy and effectiveness of different applications.[44] This can be explained by the energy efficiency value such as the energy yield (mg kW^{-1} h^{-1}) at 50% conversion (G_{50}) by the following eqn (27).[45]

$$G_{50} = \frac{30 \times [C]_0 \times V \times K}{P \times \ln 2} \quad (27)$$

The highest G_{50} value was obtained from the pinhole plasma jet system using pure Ar gas (200.03 mg kW^{-1} h^{-1}), followed by the Ar + 20% N_2 (165.04 mg kW^{-1} h^{-1}) and Ar + 10% N_2 (164.83 mg kW^{-1} h^{-1}), respectively. A previous report by Hama Aziz and co-workers (2019) also reported the highest energy efficiency with Ar gas for the degradation of dichloroacetic acid using dielectric barrier discharge (DBD) which resulted in a G_{50} value of up to 1000 mg kW^{-1} h^{-1}. The input power in the literature was much higher than in our experiment which could be the reason for the large difference in value. However, similar results were obtained where the mixture of Ar + O_2 and Ar + N_2 which estimated a lower energy efficiency in comparison to the pure Ar gas plasma. The G_{50} value was higher when N_2 gas compositions were higher such as Ar + 20% N_2 : 20% O_2 (130.84 mg kW^{-1} h^{-1}), Ar + 20% N_2 : 10% O_2 (130.64 mg kW^{-1} h^{-1}), Ar + 10% O_2 (128.17 mg kW^{-1} h^{-1}), Ar + 20% O_2 (127.52 mg kW^{-1} h^{-1}), Ar + 10% N_2 : 10% O_2 (117.82 mg kW^{-1} h^{-1}) and Ar + 10% N_2 : 20% O_2 (110.04 mg kW^{-1} h^{-1}), respectively. Furthermore, the G_{50} value of the GA plasma system obtained a negative value (−5.60 mg kW^{-1} h^{-1}). This supports the aforementioned result in the previous section where the degradation of diuron was not observed in the GA plasma system. Therefore, the efficiency of different plasma systems should be considered. Plasma treatments have also been proposed as a green disinfectant in the treatment of food products as the changes to the food quality is minimal. PAS is effective in the decontamination of pesticides and microorganisms, simultaneously. The treatment of water *via* air plasma can be less time consuming than conventional methods and extremely environmentally friendly. In conventional methods, the treatment of contaminated water includes coagulation, precipitation, filtration, and disinfection where the particles are not degraded but simply removed from the contaminated water and require further treatments.

Conclusions

In this study, GA and pinhole plasma jet systems were compared for the degradation of herbicide, diuron, in DI water. The GA plasma system was able to produce nitrate and nitrite concentration in relatively higher amount than the pinhole plasma jet system. However, it was found that the GA system was not able to degrade the diuron in solution. The lowest H_2O_2 content, nitrite concentration and EC of the herbicide solution after the plasma treatment corresponded to the highest degradation percentage of the herbicide. The pinhole plasma jet was able to degrade over fifty percent of the diuron concentration within one hour. The most prominent gas for the degradation of diuron was Ar, followed by N_2 and O_2 gas, respectively. However,

further studies are needed to enhance our understanding of the toxicity of the chemical transformation products and the specific reactive species involved.

Author contributions

Chonlada Bennett and Sawanya Ngamrung; data curation, methodology, investigation, formal analysis, writing – original draft. Vithun Ano and Chanchai Umongno; hardware, resources. Sugunya Mahatheeranont, Jaroon Jakmunee, Mudtorlep Nisoa, Komgrit Leksakul and Choncharoen Sawangrat; conceptualisation, supervision, visualisation, methodology. Dheerawan Boonyawan: conceptualisation, supervision, visualisation, resources, writing – review and editing.

Conflicts of interest

There are no conflicts to declare.

Acknowledgements

This research is supported by the International Research Network Program (IRN) 2020–2023 funded by the National Research Council of Thailand (NRCT), grant number 173430/2022. The authors would like to thank the Department of Physics and Materials Science, Faculty of Science, Chiang Mai University for providing resources throughout this research. We would like to extend our gratitude to the Department of Chemistry, Faculty of Science, Chiang Mai University for providing research instrumentations. The Agriculture and Bio Plasma Technology Centre (ABPlas) at the Science and Technology Park, Chiang Mai University is hugely acknowledged for providing research equipment and laboratory facilities.

References

1 W. Laohaudomchok, N. Nankongnab, S. Siriruttanapruk, P. Klaimala, W. Lianchamroon, P. Ousap, *et al.*, Pesticide use in Thailand: current situation, health risks, and gaps in research and policy, *Hum. Ecol. Risk Assess*, 2021, **27**(5), 1147–1169.

2 M. Tudi, H. D. Ruan, L. Wang, J. Lyu, R. Sadler, D. Connell, C. Chu and D. T. Phung, Agriculture Development, Pesticide Application and Its Impact on the Environment, *Int. J. Environ. Res. Public Health*, 2021, **18**(3), 1112.

3 F. H. M. Tang, M. Lenzen, A. McBratney and F. Maggi, Risk of pesticide pollution at the global scale, *Nat. Geosci.*, 2021, **14**(4), 206–210.

4 L. B. Moreira, G. Diamante, M. Giroux, S. Coffin, E. G. Xu, D. M. de Souza Abessa, *et al.*, Impacts of Salinity and Temperature on the Thyroidogenic Effects of the Biocide Diuron in Menidia beryllina, *Environ. Sci. Technol.*, 2018, **52**(5), 3146–3155.

5 M. Ali, J.-H. Cheng and D.-W. Sun, Effect of plasma activated water and buffer solution on fungicide degradation from tomato (Solanum lycopersicum) fruit, *Food Chem.*, 2021, **350**, 129195.

6 Q. Liu, K. Wei, L. Yang, W. Xu and W. Xue, Preparation and application of a thidiazuron·diuron ultra-low-volume spray suitable for plant protection unmanned aerial vehicles, *Sci. Rep.*, 2021, **11**(1), 4998.

7 D. C. Gooddy, P. J. Chilton and I. Harrison, A field study to assess the degradation and transport of diuron and its metabolites in a calcareous soil, *Sci. Total Environ.*, 2002, **297**(1–3), 67–83.

8 B. G. Dasan, B. Onal-Ulusoy, J. Pawlat, J. Diatczyk, Y. Sen and M. Mutlu, A New and Simple Approach for Decontamination of Food Contact Surfaces with Gliding Arc Discharge Atmospheric Non-Thermal Plasma, *Food Bioprocess Technol.*, 2017, **10**(4), 650–661.

9 C. Sarangapani, N. N. Misra, V. Milosavljevic, P. Bourke, F. O'Regan and P. J. Cullen, Pesticide degradation in water using atmospheric air cold plasma, *J. Water Process Eng.*, 2016, **9**, 225–232.

10 C. Sawangrat, Y. Phimolsiripol, K. Leksakul, S.-N. Thanapornpoonpong, P. Sojithamporn, M. Lavilla, J. M. Castagnini, F. J. Barba and D. Boonyawan, Application of Pinhole Plasma Jet Activated Water against Escherichia coli, Colletotrichum gloeosporioides, and Decontamination of Pesticide Residues on Chili (Capsicum annuum L.), *Foods*, 2022, **11**(18), 2859.

11 Z. Machala, B. Tarabová, D. Sersenová, M. Janda and K. Hensel, Chemical and antibacterial effects of plasma activated water: correlation with gaseous and aqueous reactive oxygen and nitrogen species, plasma sources and air flow conditions, *J. Phys. D: Appl. Phys.*, 2019, **52**(3), 034002.

12 J.-L. Brisset and J. Pawlat, Chemical Effects of Air Plasma Species on Aqueous Solutes in Direct and Delayed Exposure Modes: Discharge, Post-discharge and Plasma Activated Water, *Plasma Chem. Plasma Process.*, 2016, **36**(2), 355–381.

13 R. Zhou, R. Zhou, P. Wang, Y. Xian, A. Mai-Prochnow, X. Lu, *et al.*, Plasma-activated water: generation, origin of reactive species and biological applications, *J. Phys. D: Appl. Phys.*, 2020, **53**(30), 303001.

14 P. Lukes, E. Dolezalova, I. Sisrova and M. Clupek, Aqueous-phase chemistry and bactericidal effects from an air discharge plasma in contact with water: evidence for the formation of peroxynitrite through a pseudo-second-order post-discharge reaction of H2O2 and HNO2, *Plasma Sources Sci. Technol.*, 2014, **23**(1), 015019.

15 N. N. Misra, K. M. Keener, P. Bourke and P. J. Cullen, Generation of In-Package Cold Plasma and Efficacy Assessment Using Methylene Blue, *Plasma Chem. Plasma Process.*, 2015, **35**(6), 1043–1056.

16 C. Bradu, K. Kutasi, M. Magureanu, N. Puač and S. Živković, Reactive nitrogen species in plasma-activated water: generation, chemistry and application in agriculture, *J. Phys. D: Appl. Phys.*, 2020, **53**(22), 223001.

17 G. Manonmani, L. Sandhiya and K. Senthilkumar, Mechanism and Kinetics of Diuron Oxidation Initiated by Hydroxyl Radical: Hydrogen and Chlorine Atom Abstraction Reactions, *J. Phys. Chem. A*, 2019, **123**, 8954–8967.

18 Y.-H. Jiang, J.-H. Cheng and D.-W. Sun, Effects of plasma chemistry on the interfacial performance of protein and polysaccharide in emulsion, *Trends Food Sci. Technol.*, 2020, **98**, 129–139.
19 N. N. Misra and C. Jo, Applications of cold plasma technology for microbiological safety in meat industry, *Trends Food Sci. Technol.*, 2017, **64**, 74–86.
20 J. J. Zhang, J. O. Jo, D. L. Huynh, R. K. Mongre, M. Ghosh, A. K. Singh, *et al.*, Growth-inducing effects of argon plasma on soybean sprouts via the regulation of demethylation levels of energy metabolism-related genes, *Sci. Rep.*, 2017, **7**(1), 41917.
21 P. Lukes and B. R. Locke, Plasmachemical oxidation processes in a hybrid gas–liquid electrical discharge reactor, *J. Phys. D: Appl. Phys.*, 2005, **38**(22), 4074.
22 C.-C. Lai, Y.-X. Deng and Y.-H. Liao, A study on the influence of gas mixtures on the property of plasma-activated water, *Plasma Process. Polym.*, 2020, **17**(2), 1900196.
23 N. Bolouki, W.-H. Kuan, Y.-Y. Huang and J.-H. Hsieh, Characterizations of a Plasma-Water System Generated by Repetitive Microsecond Pulsed Discharge with Air, Nitrogen, Oxygen, and Argon Gases Species, *Appl. Sci.*, 2021, **11**(13), 6158.
24 T. Takamatsu, K. Uehara, Y. Sasaki, H. Miyahara, Y. Matsumura, A. Iwasawa, *et al.*, Investigation of reactive species using various gas plasmas, *RSC Adv.*, 2014, **4**(75), 39901–39905.
25 C. Sarangapani, L. Scally, M. Gulan and P. J. Cullen, Dissipation of Pesticide Residues on Grapes and Strawberries Using Plasma-Activated Water, *Food Bioprocess Technol.*, 2020, **13**(10), 1728–1741.
26 R. Moutiq, S. K. Pankaj, Z. Wan, A. Mendonca, K. Keener and N. N. Misra, Atmospheric Pressure Cold Plasma as a Potential Technology to Degrade Carbamate Residues in Water, *Plasma Chem. Plasma Process.*, 2020, **40**(5), 1291–1309.
27 H. D. Burrows, L. M. Canle, J. A. Santaballa and S. Steenken, Reaction pathways and mechanisms of photodegradation of pesticides, *J. Photochem. Photobiol., B*, 2002, **67**(2), 71–108.
28 J. Feng, Z. Zheng, Y. Sun, J. Luan, Z. Wang, L. Wang, *et al.*, Degradation of diuron in aqueous solution by dielectric barrier discharge, *J. Hazard. Mater.*, 2008, **154**(1), 1081–1089.
29 M. Canle López, M. I. Fernández, S. Rodríguez, J. A. Santaballa, S. Steenken and E. Vulliet, Mechanisms of Direct and TiO2-Photocatalysed UV Degradation of Phenylurea Herbicides, *ChemPhysChem*, 2005, **6**(10), 2064–2074.
30 R. C. T. Temgoua, U. Bussy, D. Alvarez-Dorta, N. Galland, J. Hémez, I. K. Tonlé, *et al.*, Simulation of the environmental degradation of diuron (herbicide) using electrochemistry coupled to high resolution mass spectrometry, *Electrochim. Acta*, 2020, **352**, 136485.
31 S. Giacomazzi and N. Cochet, Environmental impact of diuron transformation: a review, *Chemosphere*, 2004, **56**(11), 1021–1032.
32 S. Meephon, T. Rungrotmongkol, S. Puttamat, S. Praserthdam and V. Pavarajarn, Heterogeneous photocatalytic degradation of diuron on zinc oxide: influence of surface-dependent adsorption on kinetics, degradation pathway, and toxicity of intermediates, *J. Environ. Sci.*, 2019, **84**, 97–111.
33 J. Fenoll, M. Martínez-Menchón, G. Navarro, N. Vela and S. Navarro, Photocatalytic degradation of substituted phenylurea herbicides in aqueous semiconductor suspensions exposed to solar energy, *Chemosphere*, 2013, **91**(5), 571–578.
34 M. A. Castillo, N. Felis, P. Aragón, G. Cuesta and C. Sabater, Biodegradation of the herbicide diuron by streptomycetes isolated from soil, *Int. Biodeterior. Biodegrad.*, 2006, **58**(3), 196–202.
35 C. K. Remucal, The role of indirect photochemical degradation in the environmental fate of pesticides: a review, *Environ. Sci.: Processes Impacts*, 2014, **16**(4), 628–653.
36 J. Li, W. Zhang, Z. Lin, Y. Huang, P. Bhatt and S. Chen, Emerging Strategies for the Bioremediation of the Phenylurea Herbicide Diuron, *Front. Microbiol.*, 2021, **12**, 686509.
37 T. Mori, S. Sudo, H. Kawagishi and H. Hirai, Biodegradation of diuron in artificially contaminated water and seawater by wood colonized with the white-rot fungus Trametes versicolor, *J. Wood Sci.*, 2018, **64**(5), 690–696.
38 P. Lukes, B. R. Locke and J.-L. Brisset, Aqueous-Phase Chemistry of Electrical Discharge Plasma in Water and in Gas–Liquid Environments, *Plasma Chemistry and Catalysis in Gases and Liquids*, 2012, pp. 243–308.
39 C. M. G. Charoux, A. Patange, S. Lamba, C. P. O'Donnell, B. K. Tiwari and A. G. M. Scannell, Applications of nonthermal plasma technology on safety and quality of dried food ingredients, *J. Appl. Microbiol.*, 2021, **130**(2), 325–340.
40 E. Pereira, A. L. Antonio, A. Rafalski, J. C. M. Barreira, L. Barros, M. B. P. P. Oliveira, *et al.*, Electron-beam irradiation as an alternative to preserve nutritional, chemical and antioxidant properties of dried plants during extended storage periods, *LWT–Food Sci. Technol.*, 2017, **82**, 386–395.
41 P. Bourke, D. Ziuzina, L. Han, P. J. Cullen and B. F. Gilmore, Microbiological interactions with cold plasma, *J. Appl. Microbiol.*, 2017, **123**(2), 308–324.
42 S. Hati, M. Patel and D. Yadav, Food bioprocessing by non-thermal plasma technology, *Curr. Opin. Food Sci.*, 2018, **19**, 85–91.
43 K. Larsson, D. Hot, J. Gao, C. Kong, Z. Li, M. Aldén, *et al.*, Instantaneous imaging of ozone in a gliding arc discharge using photofragmentation laser-induced fluorescence, *J. Phys. D: Appl. Phys.*, 2018, **51**(13), 135203.
44 A. Shelar, A. V. Singh, P. Dietrich, R. S. Maharjan, A. Thissen, P. N. Didwal, *et al.*, Emerging cold plasma treatment and machine learning prospects for seed priming: a step towards sustainable food production, *RSC Adv.*, 2022, **12**(17), 10467–10488.
45 K.-H. H. Aziza, H. Miessner, A. Mahyar, S. Mueller, D. Kalass, D. Moeller and K.-M. Omer, Removal of dichloroacetic acid from aqueous solution using non-thermal plasma generated by dielectric barrier discharge and nano-pulse corona discharge, *Sep. Purif. Technol.*, 2019, **216**, 51–57.